

Study of $e^+e^- \rightarrow \pi^+\pi^- J/\psi$ and Observation of a Charged Charmonium-like State at Belle

Z. Q. Liu,¹⁷ C. P. Shen,^{36,*} C. Z. Yuan,¹⁷ I. Adachi,¹³ H. Aihara,⁵⁹ D. M. Asner,⁴⁶ V. Aulchenko,³ T. Aushev,²¹ T. Aziz,⁵⁴ A. M. Bakich,⁵³ A. Bala,⁴⁷ K. Belous,¹⁹ V. Bhardwaj,³⁸ B. Bhuyan,¹⁵ M. Bischofberger,³⁸ A. Bondar,³ G. Bonvicini,⁶⁵ A. Bozek,⁴² M. Bračko,^{31,22} J. Brodzicka,⁴² T. E. Browder,¹² P. Chang,⁴¹ V. Chekelian,³² A. Chen,³⁹ P. Chen,⁴¹ B. G. Cheon,¹¹ R. Chistov,²¹ K. Cho,²⁶ V. Chobanova,³² S.-K. Choi,¹⁰ Y. Choi,⁵² D. Cinabro,⁶⁵ J. Dalseno,^{32,55} M. Danilov,^{21,34} Z. Doležal,⁴ Z. Drásal,⁴ A. Drutskoy,^{21,34} D. Dutta,¹⁵ K. Dutta,¹⁵ S. Eidelman,³ D. Epifanov,⁵⁹ H. Farhat,⁶⁵ J. E. Fast,⁴⁶ M. Feindt,²⁴ T. Ferber,⁶ A. Frey,⁹ V. Gaur,⁵⁴ N. Gabyshev,³ S. Ganguly,⁶⁵ R. Gillard,⁶⁵ Y. M. Goh,¹¹ B. Golob,^{30,22} J. Haba,¹³ K. Hayasaka,³⁷ H. Hayashii,³⁸ Y. Horii,³⁷ Y. Hoshi,⁵⁷ W.-S. Hou,⁴¹ Y. B. Hsiung,⁴¹ H. J. Hyun,²⁸ T. Iijima,^{37,36} K. Inami,³⁶ A. Ishikawa,⁵⁸ R. Itoh,¹³ Y. Iwasaki,¹³ D. Joffe,²⁵ T. Julius,³³ D. H. Kah,²⁸ J. H. Kang,⁶⁷ T. Kawasaki,⁴⁴ C. Kiesling,³² H. J. Kim,²⁸ J. B. Kim,²⁷ J. H. Kim,²⁶ K. T. Kim,²⁷ M. J. Kim,²⁸ Y. J. Kim,²⁶ K. Kinoshita,⁵ J. Klucar,²² B. R. Ko,²⁷ P. Kodyš,⁴ S. Korpar,^{31,22} P. Križan,^{30,22} P. Krokovny,³ T. Kuhr,²⁴ Y.-J. Kwon,⁶⁷ J. S. Lange,⁷ S.-H. Lee,²⁷ J. Li,⁵¹ Y. Li,⁶⁴ J. Libby,¹⁶ C. Liu,⁵⁰ P. Lukin,³ D. Matvienko,³ K. Miyabayashi,³⁸ H. Miyata,⁴⁴ R. Mizuk,^{21,34} G. B. Mohanty,⁵⁴ A. Moll,^{32,55} R. Mussa,²⁰ E. Nakano,⁴⁵ M. Nakao,¹³ H. Nakazawa,³⁹ Z. Natkaniec,⁴² M. Nayak,¹⁶ E. Nedelkovska,³² N. K. Nisar,⁵⁴ S. Nishida,¹³ O. Nitoh,⁶² S. Ogawa,⁵⁶ S. Okuno,²³ S. L. Olsen,⁵¹ Y. Onuki,⁵⁹ W. Ostrowicz,⁴² C. Oswald,² P. Pakhlov,^{21,34} G. Pakhlova,²¹ H. Park,²⁸ H. K. Park,²⁸ T. K. Pedlar,⁶⁸ R. Pestotnik,²² M. Petrič,²² L. E. Piilonen,⁶⁴ M. Ritter,³² M. Röhrken,²⁴ A. Rostomyan,⁶ H. Sahoo,¹² T. Saito,⁵⁸ Y. Sakai,¹³ S. Sandilya,⁵⁴ D. Santel,⁵ T. Sanuki,⁵⁸ Y. Sato,⁵⁸ V. Savinov,⁴⁸ O. Schneider,²⁹ G. Schnell,^{1,14} C. Schwanda,¹⁸ R. Seidl,⁴⁹ D. Semmler,⁷ K. Senyo,⁶⁶ O. Seon,³⁶ M. E. Sevier,³³ M. Shapkin,¹⁹ T.-A. Shibata,⁶⁰ J.-G. Shiu,⁴¹ B. Shwartz,³ A. Sibidanov,⁵³ F. Simon,^{32,55} P. Smerkol,²² Y.-S. Sohn,⁶⁷ A. Sokolov,¹⁹ E. Solovieva,²¹ M. Starič,²² M. Steder,⁶ M. Sumihama,⁸ T. Sumiyoshi,⁶¹ U. Tamponi,^{20,63} K. Tanida,⁵¹ G. Tatishvili,⁴⁶ Y. Teramoto,⁴⁵ K. Trabelsi,¹³ T. Tsuboyama,¹³ M. Uchida,⁶⁰ S. Uehara,¹³ T. Uglov,^{21,35} Y. Unno,¹¹ S. Uno,¹³ S. E. Vahsen,¹² C. Van Hulse,¹ P. Vanhoefer,³² G. Varner,¹² K. E. Varvell,⁵³ V. Vorobyev,³ M. N. Wagner,⁷ C. H. Wang,⁴⁰ M.-Z. Wang,⁴¹ P. Wang,¹⁷ X. L. Wang,⁶⁴ M. Watanabe,⁴⁴ Y. Watanabe,²³ E. Won,²⁷ B. D. Yabsley,⁵³ J. Yamaoka,¹² Y. Yamashita,⁴³ S. Yashchenko,⁶ Y. Yook,⁶⁷ Y. Yusa,⁴⁴ C. C. Zhang,¹⁷ Z. P. Zhang,⁵⁰ V. Zhilich,³ and A. Zupanc²⁴

(The Belle Collaboration)

¹University of the Basque Country UPV/EHU, 48080 Bilbao

²University of Bonn, 53115 Bonn

³Budker Institute of Nuclear Physics SB RAS and
Novosibirsk State University, Novosibirsk 630090

⁴Faculty of Mathematics and Physics, Charles University, 121 16 Prague

⁵University of Cincinnati, Cincinnati, Ohio 45221

⁶Deutsches Elektronen-Synchrotron, 22607 Hamburg

⁷Justus-Liebig-Universität Gießen, 35392 Gießen

⁸Gifu University, Gifu 501-1193

⁹II. Physikalisches Institut, Georg-August-Universität Göttingen, 37073 Göttingen

- ¹⁰*Gyeongsang National University, Chinju 660-701*
- ¹¹*Hanyang University, Seoul 133-791*
- ¹²*University of Hawaii, Honolulu, Hawaii 96822*
- ¹³*High Energy Accelerator Research Organization (KEK), Tsukuba 305-0801*
- ¹⁴*Ikerbasque, 48011 Bilbao*
- ¹⁵*Indian Institute of Technology Guwahati, Assam 781039*
- ¹⁶*Indian Institute of Technology Madras, Chennai 600036*
- ¹⁷*Institute of High Energy Physics, Chinese Academy of Sciences, Beijing 100049*
- ¹⁸*Institute of High Energy Physics, Vienna 1050*
- ¹⁹*Institute for High Energy Physics, Protvino 142281*
- ²⁰*INFN - Sezione di Torino, 10125 Torino*
- ²¹*Institute for Theoretical and Experimental Physics, Moscow 117218*
- ²²*J. Stefan Institute, 1000 Ljubljana*
- ²³*Kanagawa University, Yokohama 221-8686*
- ²⁴*Institut für Experimentelle Kernphysik,
Karlsruher Institut für Technologie, 76131 Karlsruhe*
- ²⁵*Kennesaw State University, Kennesaw, Georgia 30144*
- ²⁶*Korea Institute of Science and Technology Information, Daejeon 305-806*
- ²⁷*Korea University, Seoul 136-713*
- ²⁸*Kyungpook National University, Daegu 702-701*
- ²⁹*École Polytechnique Fédérale de Lausanne (EPFL), Lausanne 1015*
- ³⁰*Faculty of Mathematics and Physics,
University of Ljubljana, 1000 Ljubljana*
- ³¹*University of Maribor, 2000 Maribor*
- ³²*Max-Planck-Institut für Physik, 80805 München*
- ³³*School of Physics, University of Melbourne, Victoria 3010*
- ³⁴*Moscow Physical Engineering Institute, Moscow 115409*
- ³⁵*Moscow Institute of Physics and Technology, Moscow Region 141700*
- ³⁶*Graduate School of Science, Nagoya University, Nagoya 464-8602*
- ³⁷*Kobayashi-Maskawa Institute, Nagoya University, Nagoya 464-8602*
- ³⁸*Nara Women's University, Nara 630-8506*
- ³⁹*National Central University, Chung-li 32054*
- ⁴⁰*National United University, Miao Li 36003*
- ⁴¹*Department of Physics, National Taiwan University, Taipei 10617*
- ⁴²*H. Niewodniczanski Institute of Nuclear Physics, Krakow 31-342*
- ⁴³*Nippon Dental University, Niigata 951-8580*
- ⁴⁴*Niigata University, Niigata 950-2181*
- ⁴⁵*Osaka City University, Osaka 558-8585*
- ⁴⁶*Pacific Northwest National Laboratory, Richland, Washington 99352*
- ⁴⁷*Panjab University, Chandigarh 160014*
- ⁴⁸*University of Pittsburgh, Pittsburgh, Pennsylvania 15260*
- ⁴⁹*RIKEN BNL Research Center, Upton, New York 11973*
- ⁵⁰*University of Science and Technology of China, Hefei 230026*
- ⁵¹*Seoul National University, Seoul 151-742*
- ⁵²*Sungkyunkwan University, Suwon 440-746*
- ⁵³*School of Physics, University of Sydney, NSW 2006*
- ⁵⁴*Tata Institute of Fundamental Research, Mumbai 400005*

- ⁵⁵*Excellence Cluster Universe, Technische Universität München, 85748 Garching*
⁵⁶*Toho University, Funabashi 274-8510*
⁵⁷*Tohoku Gakuin University, Tagajo 985-8537*
⁵⁸*Tohoku University, Sendai 980-8578*
⁵⁹*Department of Physics, University of Tokyo, Tokyo 113-0033*
⁶⁰*Tokyo Institute of Technology, Tokyo 152-8550*
⁶¹*Tokyo Metropolitan University, Tokyo 192-0397*
⁶²*Tokyo University of Agriculture and Technology, Tokyo 184-8588*
⁶³*University of Torino, 10124 Torino*
⁶⁴*CNP, Virginia Polytechnic Institute and State University, Blacksburg, Virginia 24061*
⁶⁵*Wayne State University, Detroit, Michigan 48202*
⁶⁶*Yamagata University, Yamagata 990-8560*
⁶⁷*Yonsei University, Seoul 120-749*
⁶⁸*Luther College, Decorah, Iowa 52101*

Abstract

The cross section for $e^+e^- \rightarrow \pi^+\pi^- J/\psi$ between 3.8 GeV and 5.5 GeV is measured with a 967 fb^{-1} data sample collected by the Belle detector at or near the $\Upsilon(nS)$ ($n = 1, 2, \dots, 5$) resonances. The $Y(4260)$ state is observed, and its resonance parameters are determined. In addition, an excess of $\pi^+\pi^- J/\psi$ production around 4 GeV is observed. This feature can be described by a Breit-Wigner parameterization with properties that are consistent with the $Y(4008)$ state that was previously reported by Belle. In a study of $Y(4260) \rightarrow \pi^+\pi^- J/\psi$ decays, a structure is observed in the $M(\pi^\pm J/\psi)$ mass spectrum with 5.2σ significance, with mass $M = (3894.5 \pm 6.6 \pm 4.5) \text{ MeV}/c^2$ and width $\Gamma = (63 \pm 24 \pm 26) \text{ MeV}/c^2$, where the errors are statistical and systematic, respectively. This structure can be interpreted as a new charged charmonium-like state.

PACS numbers: 14.40.Rt, 14.40.Pq, 13.66.Bc, 13.25.Gv

*now at Beihang University, Beijing 100191

The $Y(4260)$ state was first observed by the BaBar Collaboration in the initial-state-radiation (ISR) process $e^+e^- \rightarrow \gamma_{\text{ISR}}\pi^+\pi^-J/\psi$ [1] and then confirmed by the CLEO [2] and Belle experiments [3] using the same technique. Subsequently, a charged $Z(4430)^\pm$ charmonium-like state was reported in the $\pi^\pm\psi(2S)$ invariant mass spectrum of $B \rightarrow K\pi^\pm\psi(2S)$ [4] and two Z^\pm states were observed in the $\pi^\pm\chi_{c1}$ invariant mass distribution of $B \rightarrow K\chi_{c1}\pi^\pm$ [5]. Motivated by the striking observations of charged charmonium-like [4, 5] and bottomonium-like states [6], we investigate the existence of similar states as intermediate resonances in $Y(4260) \rightarrow \pi^+\pi^-J/\psi$ decays.

After the initial observations of the $Y(4260)$ [1–3], CLEO collected 13.2 pb^{-1} of e^+e^- data at $\sqrt{s} = 4.26 \text{ GeV}$ and investigated 16 possible $Y(4260)$ decay modes with charmonium or light hadrons in the final state [7]. An ISR analysis by the Belle experiment with 548 fb^{-1} of data collected at or near $\sqrt{s} = 10.58 \text{ GeV}$ [8] showed a significant $Y(4260)$ signal as well as an excess of $\pi^+\pi^-J/\psi$ event production near 4 GeV that could be described by a broad Breit-Wigner (BW) parameterization — the so-called $Y(4008)$. Recently, the BaBar Collaboration reported an updated ISR analysis with 454 fb^{-1} of data and a modified approach for the background description [9]; the $Y(4260)$ state was observed with improved significance, but the $Y(4008)$ structure was not confirmed. Instead, they attributed the structure below the $Y(4260)$ to exponentially falling non-resonant $\pi^+\pi^-J/\psi$ production.

In this Letter, we report cross section measurements for $e^+e^- \rightarrow \pi^+\pi^-J/\psi$ between 3.8 GeV and 5.5 GeV, and a search for structures in the $\pi^+\pi^-J/\psi$, $\pi^\pm J/\psi$, and $\pi^+\pi^-$ systems. The results are based on the full Belle data sample with an integrated luminosity of 967 fb^{-1} collected at or near the $\Upsilon(nS)$ resonances ($n = 1, 2, \dots, 5$). The Belle detector operated at the KEKB asymmetric-energy e^+e^- collider [10] and is described in detail elsewhere [11]. We use the PHOKHARA [12] program to generate signal Monte Carlo (MC) events and determine experimental efficiencies. The results reported here supersede those of Ref. [8], wherein a subset of the Belle data sample was used.

The event selection is described in Ref. [8]. We require four well reconstructed charged tracks with zero net charge. For each charged track, a likelihood \mathcal{L}_X is formed from different detector subsystems for particle hypothesis $X \in \{e, \mu, \pi, K, p\}$. Tracks with a likelihood ratio $\mathcal{R}_K = \frac{\mathcal{L}_K}{\mathcal{L}_K + \mathcal{L}_\pi} < 0.4$ are identified as pions with an efficiency of about 95%. Similar ratios are also defined for lepton-pion discrimination [13]. For electrons from $J/\psi \rightarrow e^+e^-$, one track should have $\mathcal{R}_e > 0.95$ and the other track $\mathcal{R}_e > 0.05$. For muons from $J/\psi \rightarrow \mu^+\mu^-$, at least one track should have $\mathcal{R}_\mu > 0.95$; in cases where the other track has no muon identification, in order to suppress misidentified muon tracks, the polar angles of the two muon tracks in the $\pi^+\pi^-\mu^+\mu^-$ center-of-mass (CM) frame must satisfy $|\cos\theta_\mu| < 0.7$. Events with γ conversions are removed by requiring $\mathcal{R}_e < 0.75$ for the $\pi^+\pi^-$ candidate tracks. Furthermore, in $J/\psi \rightarrow e^+e^-$, such events are further reduced by requiring the invariant mass of the $\pi^+\pi^-$ candidate pair to be larger than $0.32 \text{ GeV}/c^2$. Events with a total energy deposit in the electromagnetic calorimeter (ECL) above 9 GeV are removed in the $J/\psi \rightarrow e^+e^-$ mode because the MC simulation of the trigger efficiency for these Bhabha-like events does not accurately reproduce the data. There is only one combination of $\pi^+\pi^-\ell^+\ell^-$ ($\ell = e, \mu$) in each event after the above selections.

Candidate ISR events are identified by the requirement $|M_{\text{rec}}^2| < 2.0 \text{ (GeV}/c^2)^2$, where $M_{\text{rec}}^2 = (P_{CM} - P_{\pi^+} - P_{\pi^-} - P_{\ell^+} - P_{\ell^-})^2$ and P_i represents the four-momentum of the corresponding particle or composite in the e^+e^- CM frame. Clear J/ψ signals are observed in both the $J/\psi \rightarrow e^+e^-$ and $\mu^+\mu^-$ modes. We define the J/ψ signal region as $3.06 \text{ GeV}/c^2 < M(\ell^+\ell^-) < 3.14 \text{ GeV}/c^2$ (the mass resolution for lepton pairs being about $20 \text{ MeV}/c^2$), and J/ψ mass sidebands as $2.91 \text{ GeV}/c^2 < M(\ell^+\ell^-) < 3.03 \text{ GeV}/c^2$ or $3.17 \text{ GeV}/c^2 < M(\ell^+\ell^-) < 3.29 \text{ GeV}/c^2$, which are

three times as wide as the signal region.

Figure 1(a) shows the $\pi^+\pi^-\ell^+\ell^-$ invariant mass [14] distributions after all of these selection requirements are applied. Also shown in this figure are the background estimates evaluated using the normalized J/ψ -mass sidebands. Two enhancements — the $Y(4008)$ and the $Y(4260)$ — above $3.8 \text{ GeV}/c^2$ are observed, consistent with the results of Ref. [8] but in disagreement with those of Ref. [9]. Other possible background sources not included in the sidebands are found to be small from MC simulation [7]; these include (1) $\pi^+\pi^-J/\psi$ with J/ψ decays into final states other than lepton pairs and (2) XJ/ψ , with X not being a $\pi^+\pi^-$ pair, such as K^+K^- or $\pi^+\pi^-\pi^0$. Non-ISR production of $e^+e^- \rightarrow \pi^+\pi^-J/\psi$ final states, such as $e^+e^- \rightarrow \gamma\gamma^*\gamma^* \rightarrow \gamma\rho^0J/\psi$, is also estimated to be small [15]. Figure 1(b) shows the measured cross sections for $e^+e^- \rightarrow \pi^+\pi^-J/\psi$, where the error bars are statistical only.

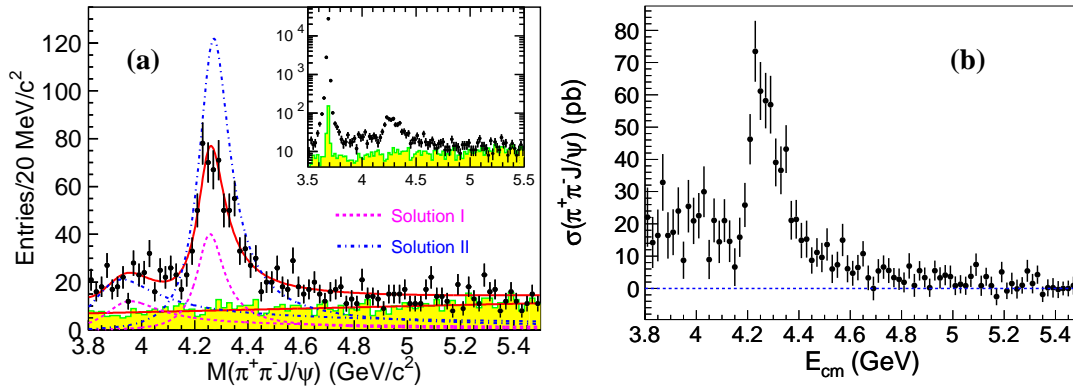


FIG. 1: (a) Invariant mass distributions of $\pi^+\pi^-\ell^+\ell^-$. Points with error bars are data, and the shaded histograms are the normalized J/ψ mass sidebands. The solid curves show the total best fit with two coherent resonances and contribution from background. The dashed curves are for solution I, while the dot-dashed curves are for solution II. The inset shows the distributions on a logarithmic vertical scale. The large peak around $3.686 \text{ GeV}/c^2$ is the $\psi(2S) \rightarrow \pi^+\pi^-J/\psi$ signal. (b) Cross section of $e^+e^- \rightarrow \pi^+\pi^-J/\psi$ after background subtraction. The errors are statistical only.

Systematic uncertainties of the cross section measurement are found to be 7.9% and 7.3% for the e^+e^- and $\mu^+\mu^-$ modes, respectively. The particle identification (PID) uncertainties, measured from pure $\psi(2S)$ events in the same data sample, are 4.7% and 3.6% for the e^+e^- and $\mu^+\mu^-$ modes, respectively. Tracking efficiency uncertainties are estimated to be 3.3% for both e^+e^- and $\mu^+\mu^-$ modes in the momentum and angular regions of interest for signal events. The uncertainties associated with the choice of the J/ψ mass window and $|M_{\text{rec}}^2|$ requirements are also estimated using pure $\psi(2S)$ events. It is found that MC efficiencies are higher than data by $(4.5 \pm 0.4)\%$ in the e^+e^- mode and $(4.1 \pm 0.2)\%$ in the $\mu^+\mu^-$ mode. The differences in efficiencies are corrected and the uncertainties in the correction factors are incorporated into the systematic errors. Overall, together with the $|M_{\text{rec}}^2|$ requirements, these uncertainties contribute 0.6% for the e^+e^- mode and 0.3% for the $\mu^+\mu^-$ mode within the J/ψ mass window. Belle measures luminosity with a precision of 1.4% using wide-angle Bhabha events. The PHOKHARA generator calculates ISR with 0.1% accuracy [12]. The dominant uncertainties due to the MC generator are from three-body decay dynamics. MC simulation with modified $\pi^+\pi^-$ invariant mass distributions weighted according to data distributions yields a 2% to 5% efficiency difference compared with a phase space $\pi^+\pi^-$ mass spectrum model. Thus, we conservatively use 5% as the systematic error due to the approximations

made in the MC event generator. According to MC simulation, the offline trigger efficiency for four-track events of the studied topology exceeds 99%. A 1.0% systematic error is included for the trigger uncertainty. The uncertainty of $\mathcal{B}(J/\psi \rightarrow \ell^+\ell^-) = \mathcal{B}(J/\psi \rightarrow e^+e^-) + \mathcal{B}(J/\psi \rightarrow \mu^+\mu^-)$ is 1.0% [16].

As a validation of our analysis, we also measure the ISR $\psi(2S)$ production rate using the same selection criteria. The cross sections are $(14.12 \pm 0.18 \pm 0.85)$ pb and $(15.13 \pm 0.11 \pm 0.79)$ pb at $\sqrt{s} = 10.58$ GeV [17] for the e^+e^- and $\mu^+\mu^-$ modes, respectively. Our measurement agrees within errors with the prediction of (14.25 ± 0.26) pb [18] using the world-average resonance parameters [16].

An unbinned maximum likelihood fit is performed to the $\pi^+\pi^-J/\psi$ mass spectrum above $3.8 \text{ GeV}/c^2$. As there are two enhancements observed, as shown in Fig. 1(a), we use the same fit strategy as in Ref. [8]. Two coherent BW functions (R_1, R_2) are used to describe the $Y(4008)$ and $Y(4260)$ structures, assuming there is no continuum production of $e^+e^- \rightarrow \pi^+\pi^-J/\psi$. In the fit, the background term is fixed at the level obtained from a linear fit to the sideband data. The solid curves in Fig. 1(a) show the fit results. There are two solutions of equal optimum fit quality. The masses and widths of the resonances are the same for the two solutions; the partial widths to e^+e^- and the relative phase between the two resonances are different (see Table I) [19]. The fit quality is estimated using the reduced χ^2 statistic; we obtain $\chi^2/ndf = 101.6/84$, corresponding to a confidence level of 9.3%. Systematic uncertainties in the extracted values of the resonance parameters arise from the absolute energy scale, the detection efficiency, background estimation and the parameterization of the resonance models. The absolute energy uncertainty is estimated from the $\psi(2S)$ mass fit. Uncertainty in the detection efficiency does not affect the mass and width measurements, but could affect the measurement of the partial width to e^+e^- . Systematic uncertainties associated with the background contribution are estimated by varying the background level by $\pm 1\sigma$ in the fit. Resonance parameterization is studied by changing the $Y(4260)$ BW function from a parameterization with a constant width to another with a three-body phase-space-dependent function. The interference between the two resonances, $Y(4260)$ and $Y(4008)$, depends on the structure of the $\pi^+\pi^-J/\psi$ amplitude, which can be different for the two resonances. We conservatively estimate possible systematic effects by performing a fit without the interference between the $Y(4008)$ and the $Y(4260)$ and taking the difference compared to results with interference as the corresponding systematic error. All of these contributions are summarized in Table I. The measured mass, width and the product $\Gamma_{ee}\mathcal{B}(R_1 \rightarrow \pi^+\pi^-J/\psi)$ are consistent within statistics with the previous results [8, 20].

Figure 2 shows the Dalitz plot for events in the $Y(4260)$ signal region ($4.15 \text{ GeV}/c^2 < M(\pi^+\pi^-J/\psi) < 4.45 \text{ GeV}/c^2$), where we observe structures in the $\pi^+\pi^-$ and π^+J/ψ systems. The inset is for the events in the J/ψ -mass sidebands, where no obvious structures are observed in the non- $\pi^+\pi^-J/\psi$ background events.

Figure 3 shows a projection of the $M(\pi^+\pi^-)$, $M(\pi^+J/\psi)$ and $M(\pi^-J/\psi)$ invariant mass distributions for events in the $Y(4260)$ signal region. Background contributions are estimated from the normalized J/ψ mass sidebands. There are $f_0(980)$, $f_0(500)$ and non-resonant S-wave amplitudes in the $\pi^+\pi^-$ mass spectrum. In the $\pi^\pm J/\psi$ mass spectrum, there is a significant peak around $3.9 \text{ GeV}/c^2$ (called the $Z(3900)^\pm$ hereafter) that we interpret as evidence for an exotic charmonium-like state decays into $\pi^\pm J/\psi$; the broader peak near $3.5 \text{ GeV}/c^2$ is a reflection of the $Z(3900)^\pm$, as confirmed by MC simulation. The pure $\pi^+\pi^-$ S-wave amplitudes that describe the $\pi^+\pi^-$ invariant mass distribution well cannot reproduce the structure at $3.9 \text{ GeV}/c^2$ in the $\pi^\pm J/\psi$ mass spectra, as shown in Fig. 3 with the open histograms.

An unbinned maximum likelihood fit is performed to the distribution of $M_{\max}(\pi J/\psi)$, the

TABLE I: Results of the fits to the $\pi^+\pi^-J/\psi$ mass spectrum with two coherent resonances. $M(R_i)$, $\Gamma_{\text{tot}}(R_i)$ and $\Gamma_{ee}\mathcal{B}(R_i \rightarrow \pi^+\pi^-J/\psi)$, $i = 1, 2$ represent the mass (in MeV/c^2), total width (in MeV/c^2) and product of the branching ratio for the decay into $\pi^+\pi^-J/\psi$ and the e^+e^- partial width (in eV/c^2) for the two resonances, respectively. The parameter ϕ (in degrees) is the relative phase between the two resonances. The first and second errors are statistical and systematic, respectively.

Parameters	Solution I	Solution II
$M(R_1)$	$3890.8 \pm 40.5 \pm 11.5$	
$\Gamma_{\text{tot}}(R_1)$	$254.5 \pm 39.5 \pm 13.6$	
$\Gamma_{ee}\mathcal{B}(R_1 \rightarrow \pi^+\pi^-J/\psi)$	$(3.8 \pm 0.6 \pm 0.4) (8.4 \pm 1.2 \pm 1.1)$	
$M(R_2)$	$4258.6 \pm 8.3 \pm 12.1$	
$\Gamma_{\text{tot}}(R_2)$	$134.1 \pm 16.4 \pm 5.5$	
$\Gamma_{ee}\mathcal{B}(R_2 \rightarrow \pi^+\pi^-J/\psi)$	$(6.4 \pm 0.8 \pm 0.6) (20.5 \pm 1.4 \pm 2.0)$	
ϕ	$59 \pm 17 \pm 11$	$-116 \pm 6 \pm 11$

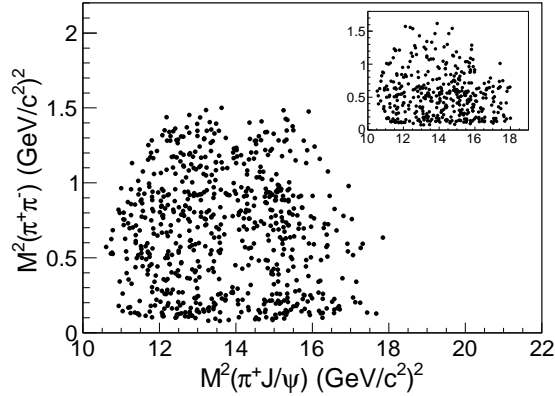


FIG. 2: Dalitz plot for $Y(4260) \rightarrow \pi^+\pi^-J/\psi$ decays for $4.15 \text{ GeV}/c^2 < M(\pi^+\pi^-J/\psi) < 4.45 \text{ GeV}/c^2$. The inset shows background events from the J/ψ -mass sidebands (not normalized).

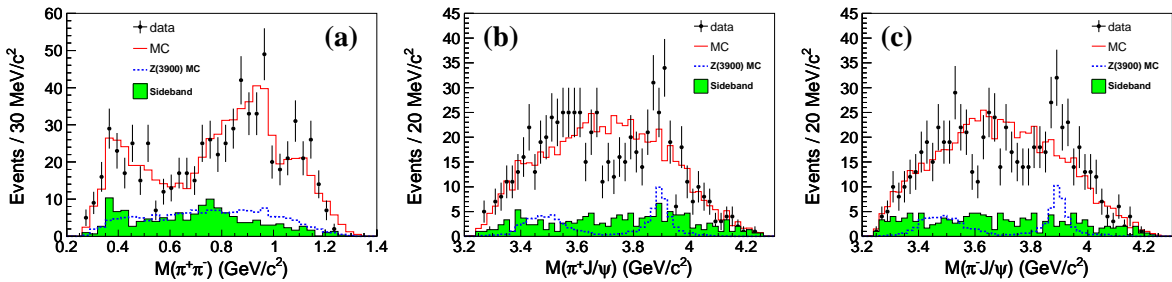


FIG. 3: Invariant mass distributions of (a) $\pi^+\pi^-$, (b) π^+J/ψ and (c) π^-J/ψ for events in the $Y(4260)$ signal region. Points with error bars represent data, shaded histograms are normalized background estimates from the J/ψ -mass sidebands, solid histograms represent MC simulations of $\pi^+\pi^-$ amplitudes [21] (normalized J/ψ -mass sideband events added) and dashed histograms are MC simulation results for a $Z(3900)^\pm$ signal

maximum of $M(\pi^+ J/\psi)$ and $M(\pi^- J/\psi)$. The signal shape is parameterized as an S-wave BW function convolved with a Gaussian whose mass resolution is fixed at the MC-estimated value of 7.4 MeV, and the background is approximated by a cubic polynomial. The mass-dependent efficiency is also included in the fit. Figure 4 shows the fit results. The fit yields $159 \pm 49 \pm 7 Z(3900)^\pm$ events, with a mass of $(3894.5 \pm 6.6 \pm 4.5) \text{ MeV}/c^2$ and a width of $(63 \pm 24 \pm 26) \text{ MeV}/c^2$, where the errors are statistical and systematic, respectively. The largest contributions to the systematic uncertainties arise from the parameterization of the signal and background shapes, the mass resolution and mass calibrations. The statistical significance of the $Z(3900)^\pm$ state is found to be 5.5σ in the nominal fit, and is larger than 5.2σ in all alternate fits used for systematic checks with different background shapes, fit ranges and BW resonant models. The significance is calculated by comparing the logarithmic likelihoods with and without the $Z(3900)^\pm$ signal, and including the change of the number of parameters in the fits. From the signal yields and the MC-simulated efficiencies, we obtain the ratio of the production rates $\frac{\mathcal{B}(Y(4260) \rightarrow Z(3900)^\pm \pi^\mp) \mathcal{B}(Z(3900)^\pm \rightarrow \pi^\pm J/\psi)}{\mathcal{B}(Y(4260) \rightarrow \pi^+ \pi^- J/\psi)} = (29.0 \pm 8.9)\%$, where the error is statistical only [22]. We test the hypothesis that interference between the S- and D-waves in the $\pi^+ \pi^-$ system might produce a structure similar to the enhancement observed in data. Although the statistics do not allow us to fully explore the Dalitz plot via an amplitude analysis, we find that these partial waves alone cannot produce a $\pi^\pm J/\psi$ invariant mass peak near $3.9 \text{ GeV}/c^2$ [21]. Inclusion of a $Z(3900)^\pm$ with the mass and width determined above significantly improves the agreement between predicted and observed Dalitz plot distributions.

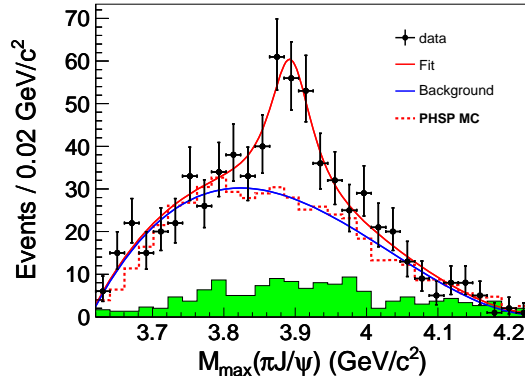


FIG. 4: Unbinned maximum likelihood fit to the distribution of the $M_{\max}(\pi J/\psi)$. Points with error bars are data, the curves are the best fit, the dashed histogram is the phase space distribution and the shaded histogram is the non- $\pi^+ \pi^- J/\psi$ background estimated from the normalized J/ψ sidebands.

In summary, the cross section of $e^+ e^- \rightarrow \pi^+ \pi^- J/\psi$ is measured from 3.8 GeV to 5.5 GeV. The $Y(4260)$ resonance is observed and its resonant parameters are determined. In addition, the $Y(4008)$ state is confirmed. The intermediate states in $Y(4260) \rightarrow \pi^+ \pi^- J/\psi$ decays are also investigated. A $Z(3900)^\pm$ state with a mass of $(3894.5 \pm 6.6 \pm 4.5) \text{ MeV}/c^2$ and a width of $(63 \pm 24 \pm 26) \text{ MeV}/c^2$ is observed in the $\pi^\pm J/\psi$ mass spectrum with a statistical significance larger than 5.2σ . This state is close to the $D\bar{D}^*$ mass threshold; however, no enhancement is observed near the $D^* \bar{D}^*$ mass threshold. As the $Z(3900)^\pm$ state has a strong coupling to charmonium and is charged, we conclude it cannot be a conventional $c\bar{c}$ state.

We thank the KEKB group for excellent operation of the accelerator; the KEK cryogenics group for efficient solenoid operations; and the KEK computer group, the NII, and PNNL/EMSL for valuable computing and SINET4 network support. We acknowledge support from MEXT, JSPS and Nagoya's TLPRC (Japan); ARC and DIISR (Australia); NSFC (China); MSMT (Czechia);

DST (India); INFN (Italy); MEST, NRF, GSDC of KISTI, and WCU (Korea); MNiSW and NCN (Poland); MES and RFAAE (Russia); ARRS (Slovenia); SNSF (Switzerland); NSC and MOE (Taiwan); and DOE and NSF (USA). This work is supported partly by a Grant-in-Aid from MEXT for Science Research on Innovative Areas (“Elucidation of New Hadrons with a Variety of Flavors”) and JSPS KAKENHI Grant No. 24740158.

Note added.— As we were preparing to submit this paper, we became aware of a paper from the BESIII Collaboration [23] that also reports on the $Z(3900)^\pm$.

-
- [1] B. Aubert *et al.* (BaBar Collaboration), Phys. Rev. Lett. **95**, 142001 (2005).
[2] Q. He *et al.* (CLEO Collaboration), Phys. Rev. D **74**, 091104(R) (2006).
[3] K. Abe *et al.* (Belle Collaboration), hep-ex/0612006.
[4] S. K. Choi *et al.* (Belle Collaboration), Phys. Rev. Lett. **100**, 142001 (2008).
[5] R. Mizuk *et al.* (Belle Collaboration), Phys. Rev. D **78**, 072004 (2008).
[6] A. Bondar *et al.* (Belle Collaboration), Phys. Rev. Lett. **108**, 122001 (2012).
[7] T. E. Coan *et al.* (CLEO Collaboration), Phys. Rev. Lett. **96**, 162003 (2006).
[8] C. Z. Yuan *et al.* (Belle Collaboration), Phys. Rev. Lett. **99**, 182004 (2007).
[9] J. P. Lees *et al.* (BaBar Collaboration), Phys. Rev. D **86**, 051102(R) (2012).
[10] S. Kurokawa and E. Kikutani, Nucl. Instrum. Methods Phys. Res., Sect. A **499**, 1 (2003), and other papers included in this volume; T. Abe *et al.*, Prog. Theor. Exp. Phys. (2013) 03A001 and following articles up to 03A011.
[11] A. Abashian *et al.* (Belle Collaboration), Nucl. Instrum. Methods Phys. Res., Sect. A **479**, 117 (2002); also see detector section in J. Brodzicka *et al.*, Prog. Theor. Exp. Phys. (2012) 04D001.
[12] G. Rodrigo, H. Czyż, J. H. Kühn and M. Szopa, Eur. Phys. J. C **24**, 71 (2002).
[13] K. Hanagaki *et al.*, Nucl. Instrum. Methods Phys. Res., Sect. A **485**, 490 (2002); A. Abashian *et al.*, Nucl. Instrum. Methods Phys. Res., Sect. A **491**, 69 (2002).
[14] In the paper, $M(\pi^+\pi^-\ell^+\ell^-) - M(\ell^+\ell^-) + M(J/\psi)$ is used instead of the invariant mass of the four final state particles to improve the mass resolution. Here $M(J/\psi)$ is the nominal mass of the J/ψ .
[15] K. Zhu, C. Z. Yuan and R. G. Ping, Phys. Rev. D **78**, 036004 (2008).
[16] J. Beringer *et al.* (Particle Data Group), Phys. Rev. D **86**, 010001 (2012).
[17] The cross sections are measured to be $(13.79 \pm 0.44 \pm 0.83)$ pb and $(13.33 \pm 0.25 \pm 0.70)$ pb at $\sqrt{s} = 10.87$ GeV, $(16.75 \pm 0.85 \pm 1.01)$ pb and $(16.63 \pm 0.54 \pm 0.87)$ pb at $\sqrt{s} = 10.02$ GeV, for the e^+e^- and $\mu^+\mu^-$ modes, respectively. Our measurements agree with the predictions of (13.42 ± 0.25) pb at 10.87 GeV, and (16.03 ± 0.29) pb at 10.02 GeV [18] within errors.
[18] E. A. Kuraev and V. S. Fadin, Sov. J. Nucl. Phys. **41**, 466 (1985) [Yad. Fiz. **41**, 733 (1985)].
[19] Considering the correlation between $\Gamma_{ee}\mathcal{B}(R \rightarrow \pi^+\pi^-J/\psi)$ and Γ_{tot} , we get $\mathcal{B}_{ee}\mathcal{B}(R \rightarrow \pi^+\pi^-J/\psi) = (1.5 \pm 0.3 \pm 0.2) \times 10^{-8}$ and $(4.8 \pm 0.6 \pm 0.5) \times 10^{-8}$ for R_1 and R_2 , respectively, for solution I; and $\mathcal{B}_{ee}\mathcal{B}(R \rightarrow \pi^+\pi^-J/\psi) = (3.3 \pm 0.7 \pm 0.5) \times 10^{-8}$ and $(15.3 \pm 1.4 \pm 1.5) \times 10^{-8}$ for R_1 and R_2 , respectively, for solution II, where the first and second errors are statistical and systematic, respectively.
[20] A smaller systematic error is obtained because we no longer use a BW with a phase-space-dependent total width to parameterize R_1 .
[21] We perform a partial wave analysis with $f_0(500)$, $f_0(980)$, non-resonant S-wave, and $f_2(1270)$ amplitudes, and find that the S-wave contributions dominate. The MC distributions with fit parameters are shown in Fig. 3 with open histograms.

- [22] The fraction of $Z(3900)^\pm$ events is obtained from a one-dimensional fit to the $M_{\max}(\pi J/\psi)$ distribution without including possible interference with other amplitudes. For a more precise determination of this fraction, a full partial wave analysis with more statistics would be required.
- [23] M. Ablikim *et al.* (BESIII Collaboration), arXiv:1303.5949.